EUROPEAN ORGANIZATION FOR NUCLEAR RESEARCH

NP Internal Report 61 - 14
Internal Circulation Only
Not for Publication.

COUNTING RATE IN THE PLANNED EXPERIMENT TO DETECT NEUTRINO INDUCED REACTIONS, II

by G. von Dardel

1. Introduction

In a previous report[1)] the expected rate of neutrino induced events was calculated under conditions which approximately correspond to the present situation of the neutrino experiment. The calculations indicated that the aperture of the coils of the next magnet unit after the target, through which the pions have to pass, reduces the event rate in detectors involving only a few tons of material to values which must be regarded as unacceptably low for a successful experiment on high energy neutrinos.

In this report, the method of calculation is generalized to some extent, so as to provide a basis for easy and rapid calculation. The effect of various changes to the geometry will be discussed, and the effect of some features not taken into account in the last report will be considered.

2. Standard Conditions

The daily rate of neutrino induced events of a particular type is given[2] by formula (1) of reference 2.

$$R^{i} = \eta_1 \eta_2 \eta_3 \; I_p Q N \frac{W}{2} \frac{1}{L^2} \int_0^{\infty} dp\, \sigma^{i}_{eff}(p) \left(1 - e^{-s/\lambda p}\right) A(p) \times f(p) \qquad (1)$$

where

η_1	is the proportion of useful detector time.
η_2	is the target efficiency.
η_3	is the proportion of useful machine time.
I_p	is the number of circulating protons per burst.
Q	is the theoretical number of bursts per day.
W	is the effective weight of the detector, assumed to consist of equal numbers of neutrons and protons.
N	is Avogadro's number.
L	is the target to detector distance.
$\sigma^{i}_{eff}(p)$	is the effective cross-section per nucleon for neutrinos produced from the decay of pions of momentum p, to produce an event of type "i". $\sigma^{i}_{eff}(p)$ depends also on the geometry as described in reference 1.
$\left(1-e^{-s/\lambda p}\right)$	is the decay probability over a distance s for pions of momentum p $(\lambda = 55 \text{ m } (\text{GeV/c})^{-1})$.
$A(p)$	is the momentum dependent enhancement factor for pions due to the focusing and defocusing effect of the fringing field.
$f(p)$	is the differential pion production per GeV/c and steradian, per proton interacting in the target.

Since the main purpose of the present paper is to study the effect of different geometric arrangements, the values of the following parameters will be fixed:

$\eta_1 \eta_2 \eta_3 \; I_p = 10^{11}$ effective protons per burst. This amounts to the same assumption as done by Krienen, Salmeron and Steinberger[2], and by Salmeron[3], who took $\eta_1 \eta_2 \eta_3 = 1/3$ and $I_p = 3 \cdot 10^{11}$ protons per burst.

Q = 28.800 bursts/day at 24 GeV machine energy.

N = $0.602 . 10^{24}$ nucleons/gramme.

w = 10^6 gramme, i.e. the event rate is given per ton of detector.

L = 51 m.

s = 25 m.

With these values the constant in front of the integral in eq. (1) becomes

$$\frac{1}{3} \times 10^{38} \text{ cm}^{-2}.$$

The number f(p) of pions per interaction produced per steradian and GeV/c momentum band is calculated by J. von Behr and R. Hagedorn[4)] for production angles of 0°, 5° and 10° with respect to the 25 GeV proton beam, and are given in Fig.1. The dotted spectrum refers to the spectrum of positive pions[3)], produced at angles such that, after the fringing field, they emerge at 6°. Since the positive pions are deflected towards the machine, the production angles are then larger than 6°, particularly at low momenta.

For the elementary cross-sections $\sigma_{\nu}(p_{\nu})$ for producing neutrino events, we take the same values as Krienen, Salmeron and Steinberger.[2)] For convenience sake, these data are redrawn on a larger scale in Fig. 2. The curves do not, of course, claim to be more than those of reference2.

The length s of the decay path, in which pions decay to neutrinos before they are absorbed in the shielding, is taken as 25 m. This is somewhat longer than the value, 20 m, taken in reference 1, but corresponds better to the present situation.

3. The Effective Cross-section

The "effective cross-section" for a given pion momentum $p, \sigma_{eff}(p)$, was originally introduced by Krienen, Salmeron and Steinberger[2)] as the elementary neutrino cross-section of Fig. 2 averaged over neutrino momenta between zero and the maximum value 0.425 p. Their definition applies to the case when the whole area around the detector is uniformly "illuminated" by the pion flux (assuming they did not decay or were absorbed). The neutrino flux will be reduced if the uniformly illuminated area is limited to a certain area around the detector, while no pions strike outside this area, as is obtained in practice if the pion beam is limited by an aperture. The neutrino flux at the detector will receive contributions from the pion decays, a distance L_1 in front of the detector if the extrapolated pion path traverses the detector plane on a circle of radius $L_1 \cdot tg\,\Theta$ around the detector and the neutrino is sent off at an angle Θ with respect to the pion. If $\alpha(\Theta)$ is the fraction of the periphery of this circle lying inside the illuminated area, one can define for each geometry and pion momentum p, an effective neutrino cross-section

$$\sigma_{eff}(p) = \frac{1}{2} \int_{-1}^{+1} d(\cos\Theta^*) \sigma_\nu (p_\nu) \cdot \alpha(\Theta) \qquad (2)$$

where Θ^* is the decay angle in the rest frame of the pion, which, for relativistic pions, is related to the laboratory angle Θ by

$$tg\,\Theta = \frac{m_\pi c}{p} \sqrt{\frac{1-\cos\Theta^*}{1+\cos\Theta^*}} \qquad (3)$$

and p_ν is the neutrino momentum

$$p_\nu = .213\, p\,(1 + \cos\Theta^*) \qquad (4)$$

The simplest geometry to consider is the case of a circular region uniformly illuminated by the pion flux. For the calculation of the neutrino event rate at the centre of the circle, the relevant cross-section is given by eq. (2) with

$$\alpha(\Theta) = 1 \qquad \Theta < \Theta_o \tag{5a}$$
$$\alpha(\Theta) = 2 \qquad \Theta > \Theta_o \tag{5b}$$

where Θ_o is the angle subtended by the radius of the circle, as seen from the decay point. This effective cross-section $\sigma^c_{eff}(p,x)$ where the superscript 'c' stands for 'circle' is shown as a function of $x = tg\,\Theta_o$, in Fig. 3.

Another simple geometry, already discussed, for a special case in reference 1, is the case of an illuminated band of uniform width, subtending the angle $2\Theta_o$ from the decay point. For the calculation of the neutrino event rate on the centre line, the relevant effective cross-section is given by eq. (2) and (5a) with (5b) replaced by

$$\alpha(\Theta) = \frac{2}{\pi} \arcsin \Theta/\Theta_o \qquad \Theta > \Theta_o \tag{5c}$$

This effective cross-section, $\sigma^b_{eff}(p,x)$, where the superscript 'b' stands for 'band', is given as a function of pion momentum and $x = tg\Theta_o$ in Fig. 4.

A third case of some importance is when the whole area around the detector is uniformly illuminated but the detecting equipment is only able to record events due to neutrinos with a momentum higher than a certain minimum value. To a minimum neutrino momentum corresponds a maximum decay angle by eq. (3) and (4). This relation is shown in Fig. 5. The case of an energy cut off can therefore be calculated using the effective cross-sections of Fig. 3 for circular geometry.

With the two simple geometries many other geometries can be constructed by superposition. In this way it is possible to take account of nonuniform illumination in the circular or bandshaped geometry and a gradually falling detector efficiency with decreasing neutrino momentum.

4. Effect of the Finite Decay Path

In the following calculations the effect of the geometry will be evaluated on the assumption that all pions decay at the centre of the decay path, but it will first be demonstrated that the error made by this approximation is small.

For a given pion momentum, p, the true neutrino event rate, R_d, for pion decays distributed over the whole decay path, s, is:

$$R_d = \text{const} \int_{-s/2}^{+s/2} e^{-(\frac{s}{2} + y)/\lambda p} \cdot \sigma_{eff}(p,\Theta_o(y))\,dy \qquad (6)$$

This has to be compared with the approximate value one obtains if one uses for σ_{eff} its value $\sigma_{eff}(p, \Theta_o(0))$ at the centre of the decay path.

$$R_c = \text{const}\ (1 - e^{-s/\lambda p})\ \sigma_{eff}\ (p,\Theta_o(0)) \qquad (7)$$

$\sigma^i_{eff}(p,\Theta_o)$ varies with the angle Θ_o over a certain range proportional to Θ_o^{μ}. For small values of Θ_o, the exponent μ is one (linear dependence on $tg\,\Theta_o$) for 'band' geometry, and two (quadratic dependence) for circular geometry. With increasing values of Θ_o, μ drops to zero. Θ_o is inversely proportional to the distance to the decay point.

Introducing the power law behaviour in eq. (6) and (7), it is easy to show, by series expansion, that the error introduced by the approximative formula (7) is

$$\frac{R_d - R_c}{R_c} = \frac{\mu}{3} \left(\frac{s}{2L_1}\right)^2 \left[\left(\frac{\mu+1}{2}\right) - \frac{L_1}{\lambda p} \right] \qquad (8)$$

where L_1 is the distance between detector and the centre of the decay path. For the present version of the neutrino experiment for which $L_1 = 51 - \frac{25}{2} = 37.5$ m and s = 25 m the error, for any momentum, is smaller than 3.5% for any 'band' geometry and 10% for any circular geometry. For the geometry of the actual experimental conditions, and averaged over the momentum spectra of Fig. 2, the error is much smaller and completely negligible with respect to other uncertainties.

5. Detailed Calculations

With the diagrams of Fig. 3 and 5, it is easy to calculate the expected event rate under standard conditions by eq. (1). For these calculations the integral was evaluated by Simpson's formula.

Contrary to what was the case in the preliminary calculations,[1] the contribution of the pion spectrum above 7 GeV/c has been approximately taken into account by assuming that[5] the integrand in eq. (1) decreases exponentially in the high momentum range. Similarly the range below 1 GeV/c was taken into account by assuming an integrand increasing as p^3 in this range. The contributions from these extrapolations are less than 10% of the total integral.

All data given in the following refer to the standard conditions discussed previously, i.e. daily rate of elastic events of one kind for 10^{11} interactions per burst, per ton of sensitive material.

Fig. 6 gives the expected counting rate without aperture limitation or fringing field as a function of production angle, using the spectra of Fig. 2 as predicted by von Behr and Hagedorn[4]. For this case $\sigma_{eff}(p_\nu)$ is identical with those of reference 2.

In the same diagram is shown, at an angle of 6^o, the event rate one obtains if the dotted spectrum of Fig. 1 is used instead of the Hagedorn spectrum. As explained previously this spectrum corresponds to an emission angle of 6^o after the fringing field; and thus an effective production angle which for positive particles is somewhat larger. It is seen, in fact, that the direct effect of the fringing field is to reduce the event rate by 14%, and that a production angle of 8.3^o without fringing field would give the same event rate.

For practical purposes this value is not so interesting since it only takes into account the shift of the production angles to larger values due to the fringing field, but not the focusing and defocusing effects nor the aperture limitation introduced by the iron yoke and the coils which produce the fringing field. These were taken into account for the first time in Ref. 1 which gives a value of 0.045 for the neutrino event rate for one reaction per ton, day and 10^{11} interactions per burst. The present calculations differ from those in reference 1 in the following respects:

i) the decay length is 25 m instead of 20 m.

ii) the width of the illuminated band at the detector is determined by the coil distance, 16 cm at a distance of 2.3 m from the target instead of 15 cm at 2.5 m, as in reference 1.

iii) The decay path is divided in two parts. For the first 1.6 m before the pions enter the next magnet unit, the event rate was calculated for a production angle equal to the observation angle, 6^o, and with no aperture limitation or focusing effect of the fringing field, whereas for the last 23.5 m the calculations were performed as in reference 1. For this part the focusing and defocusing factors of the fringing field were the same as those given in Table 1 of reference 1.

The contributions to the neutrino event rate, again per reaction, day, ton and 10^{11} interactions per burst, is 0.010 for the first 1.5 m of the decay path and 0.065 for the last part, or a total rate of 0.075. The increase with respect to the previous value is mainly due to the longer decay path.

Fig. 7 gives the effect of a slit or circular aperture close to the target, expressed by the value $x = \mathrm{tg}\,\Theta_o$. Θ_o is the angle under which the half width of the illuminated band or radius of illuminated circle at the detector is seen from the decay point. For the calculations of these curves the pion spectrum of Fig.1 for 5^o production angle has been used.

Fig. 8 gives, also for 5^o production angle, the dependence of the event rate on the minimum detectable neutrino momentum.

6. Possible Improvements

Even with the less pessimistic assumptions of the present report, the estimated neutrino event rate is smaller than the one calculated by Salmeron[3)] by a factor 4 - 5. Most of this factor is due to the fact that the vertical enhancement of the fringing field is destroyed almost completely by the divergence between neutrino and pion directions.

The calculated value is lower than the value one would get if the fringing field or aperture limitation could be removed. Three effects, namely the aperture limitation in the vertical direction set by the coils of the following magnet, the horizontal defocusing of the fringing field, and the deflection of the pions towards smaller angles, coupled with the peaked angular distribution in the forward direction, give a reduction of about 15% each to give a total reduction of 0.65 (Fig.6).

Various methods have been suggested to get around these effects. A magnetic channel around the pion beam would remove the effect of the fringing field, but the vertical aperture limitation would still subsist, and the magnetic channel would also limit the horizontal aperture. A practical design might give a circular aperture with the size corresponding to $tg\,\Theta_o = 0.035$. For 5^o production angle, the expected event rate is 0.085 according to Fig.7, only very slightly higher than without the channel.

If the machine is modified to provide a long straight section after the target, the pion beam would go through a much weaker fringing field, and it might be justifiable to neglect its effect. However, the beam would still not clear the coils of the next magnet section completely. The aperture of the coils will correspond to a value $x = tg\,\Theta_o$ of 0.035. With this value we find for an infinite slit from Fig. 7 an event rate of 0.096. This value is certainly pessimistic, since the coils soon cease to be an obstruction for pions going off at large angles from the target. An optimistic estimate is obtained if we assume that the slit extends only to the right, while to the left of the central trajectory, there is no aperture limitation at all. This probable optimistic assumption leads to an expected event rate 0.120, which is the average between the value for an infinite slit and for no aperture. This value is valid for a production angle of 5^o, and at the actual angle of 6^o, a 5% lower event rate is expected. The gain with respect to the present case is therefore a factor 1.5.

A magnetic field may be used to sweep out particles produced at 0^o angle in an internal target to the direction of observation of the present neutrino detectors, 6^o. This method, proposed by Krienen seems technically feasible, since it has recently been demonstrated that the pulsed magnetic field does not disturb the circulating proton beam, provided that it is compesnated by a field in the inverse direction.

The field may be so arranged that it provides horizontal focusing over a certain range of angles to compensate to some extent for the horizontal defocusing in the subsequent fringing field. Together with the fringing field the kicker magnets will then form a doublet of quadrupole fields which gives a net focusing effect in both directions.

7. Maximum Obtainable Rate

For the long-term planning of the neutrino experiment at the PS, it may be interesting to investigate the limits to the rate which can be obtained.

The very maximum would be obtained if it were possible, by some very ingenious focusing system, to direct all pions produced at the target independent of momentum and production angle towards a point at the detector. Since the system is anyway quite hypothetical, we can also assume that the focusing device acts directly at the source and does not take away any decay path. With the same decay path, 25 m,and target to detector distance, 51 m, as in the previous calculations, one obtains for a Hagedorn production spectrum 12 events per day and ton under standard conditions for 10^{11} interactions in the target.

This maximum obtainable rate can of course never be obtained in practice. A more realistic case is that of a strong lens which focuses pions in a certain momentum band, p_o, to a point at the detector whereas for other momenta the focusing is not complete. The simple case of a thin lens covering an aperture of $\pm 10^o$ has been studied. The lens has been assumed to be so close to the target that it does not decrease the available decay path.

If we express the focusing power of the thin lens as the momentum value, p_o, for which the lens focuses the target on a point in the detector plane, calculations show that the event rate increases with p_o from the values .16 with no focusing to a maximum of 1.5 - 2 events when the lens focuses pions of 4 - 6 GeV/c, an improvment by a factor 10.

If the focusing action is achieved by a tangential magnetic field, as in van der Meer's[5)] magnetic horn, pions emitted at 10^o have to traverse an integrated field of 3 W/m, to be focused at 5 GeV/c.

The fact that the optimum is quite flat indicates that the one can allow different portions of the lens having different focusing power without substantially decreasing the effectiveness of the arrangement. The 'lens' may therefore have quite bad aberrations to a point where it can no more be considered as an image giving device at all, such as van der Meer's neutrino horn. The hypothetical thin lens considered in these paragraphs corresponds in fact quite closely to the van der Meer horn, which also gives an improvement in rate by a factor 10, by concentrating a 10^o cone towards the detector. If the lens action is achieved by a tangential magnetic field, an integrated field strength of 30 kgauss/m would be needed to focus 5 GeV/c particles emitted at 10^o and this is again the order of fields used in the neutrino horn.

The thin lens picture has been used in these paragraphs mainly for its mathematical simplicity, and not because it would be particularly suitable. In fact it is easy to see that a thick lens with the same focusing power will give focusing over a wider momentum band than the equivalent thin lens.

8. Conclusions

The event rate of 0.075 events per ton,and day, calculated for the present version of the neutrino experiment, makes the use of multiton detectors necessary to accumulate data at a reasonable rate. An increase of about a factor 2 which would be obtained if the influence of the fringing field and aperture limitations of the coil of the next magnet unit could be removed, would not substantially change this situation. Further increase, by as much as an additional factor 10, can only be obtained at the expense of large aperture, high field, focusing devices, such as the van der Meer neutrino horn, which require the extracted proton beam.

The conclusions are based on the prediction of statistical theory with isotropic production in the centre of mass. Measurements by M. Fidecaro et al[6)] indicate a γ ray angular distribution which is more peaked in the forward direction, below 7°, then statistical theory predicts. Some improvement in the event rate over the calculated rate could be expected in unfocused geometries due to this effect if it were possible to make full use of the pion beam produced in the forward direction. On the other hand, in the case of large aperture, focused geometries, with for example the neutrino horn, the forward angular distribution has relatively little effect, since most of the event rate is produced by particles produced at larger angles.

* *
*

Acknowledgements

The author acknowledges and is grateful for many fruitful discussions with G. Bernardini, R.A. Salmeron, H. Bingham, M. Nicolic and S. van der Meer.

REFERENCES

1) G. von Dardel, CERN NP Internal Report 61-5.

2) F. Krienen, R.S. Salmeron, J. Steinberger, PS/Int.EA 60-10.

3) R.A. Salmeron (private communication).

4) J. von Behr and R. Hagedorn, CERN 60-20 (1960).

5) S. van der Meer, CERN 61-7.

6) M. Fidecaro, G. Finocchiaro, G. Gatti, G. Giacomelli, W.C. Middelkoop, T. Yamagata (not yet published).

* *
*

Figure Captions

Fig. 1 - Momentum spectra for positive pion production in 25 GeV p-p collision, taken from Ref. 4, for several production angles in the laboratory system (solid curves). The dotted curve is the production spectrum at the target for the case of particles emerging at 6^{o} after passing through the fringing field.

Fig. 2 - Cross-section for the inverse β decay as a function of neutrino momentum (upper scale). Note the change in scale between 1.2 and 1.4 GeV/c. The lower scale and the millimeter grating give the minimum pion energy, corresponding to each neutrino momentum.

Fig. 3 - Effective cross-section per pion for neutrino events. The extrapolated pion trajectories illuminate uniformly a circular area around the detector, with the radius subtending an angle Θ_o, as seen from the decay plane of the pions as a function of pion momentum p, and $x = tg\,\Theta_o$.

Fig. 4 - Effective cross-section per pion for neutrino events. The extrapolated pion trajectories illuminate uniformly a band shaped region around the detector which subtend an angle $2\,\Theta_o$, as seen from the decay plane of the pions as a function of pion momentum p, and $x = tg\,\Theta_o$.

Fig. 5 - Relation between neutrino laboratory angle and neutrino momentum with the pion momentum as parameter.

Fig. 6 - Calculated neutrino event rate under standard conditions (see para. 2). Solid curve gives the rate per ton, day and reaction with 10^{11} p-p interactions per burst as a function of angle from the target with no aperture limitation or distortion of trajectories by the fringing field. The two points below the curve give for an angle of 6^{o} the effect of the deflecting action of the fringing field by itself (upper point), and the combined effect of the deflection, focusing and aperture limitation by the magnet coils (lower point).

Fig. 7 - Calculated neutrino event rate per ton, day and reaction for 10^{11} p-p interactions per burst at 5^{o} production angle, assuming no fringing field but with apertures in the pion beam which limit the illuminated area around the detector to a circle or a band subtending an angle $2\Theta_{o}$ from the decay plane.

* *
*

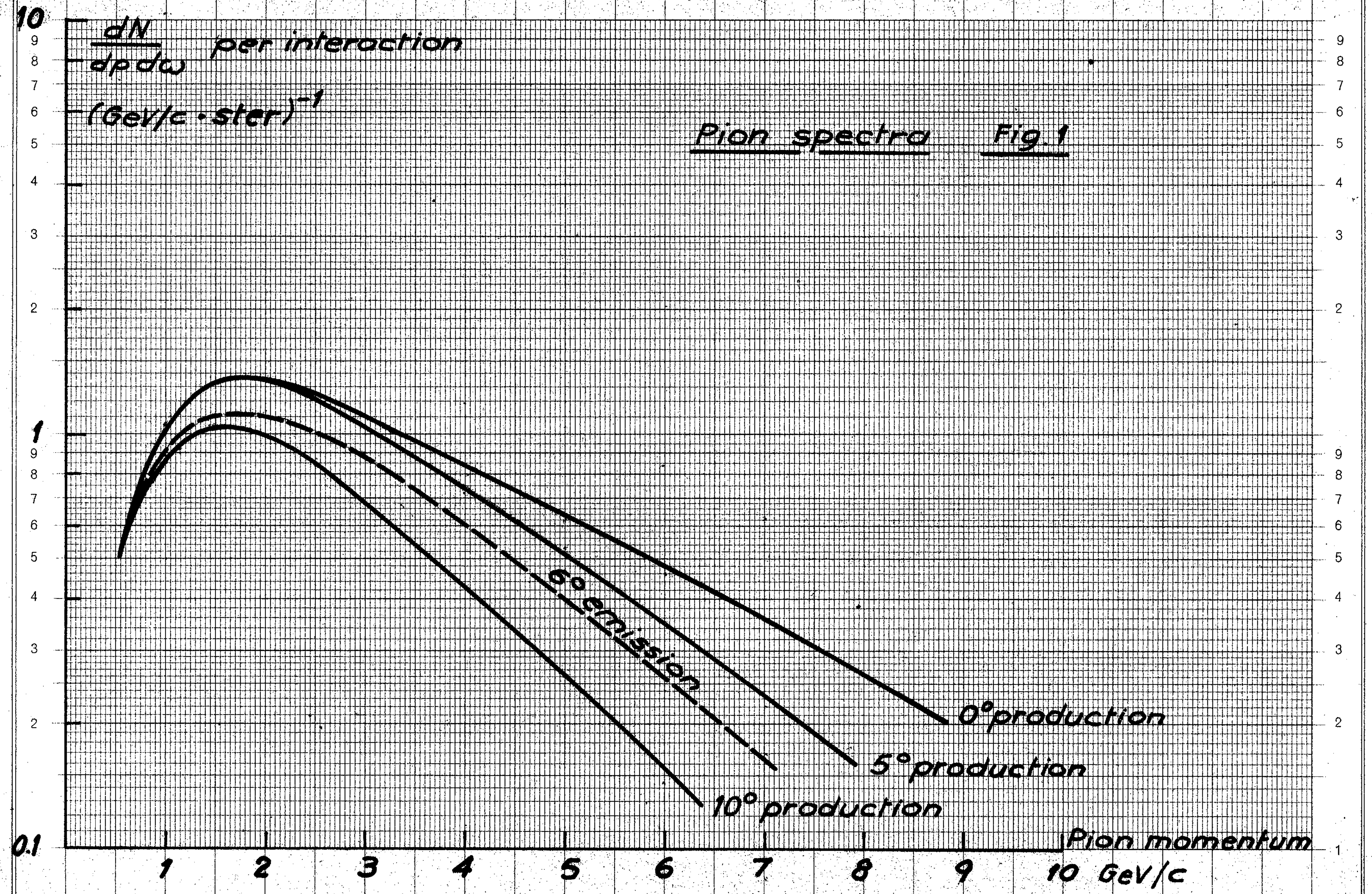

dN / dp dω per interaction
(GeV/c · ster)^-1
Pion spectra Fig. 1
0° production
5° production
6° emission
10° production
Pion momentum
10 GeV/c

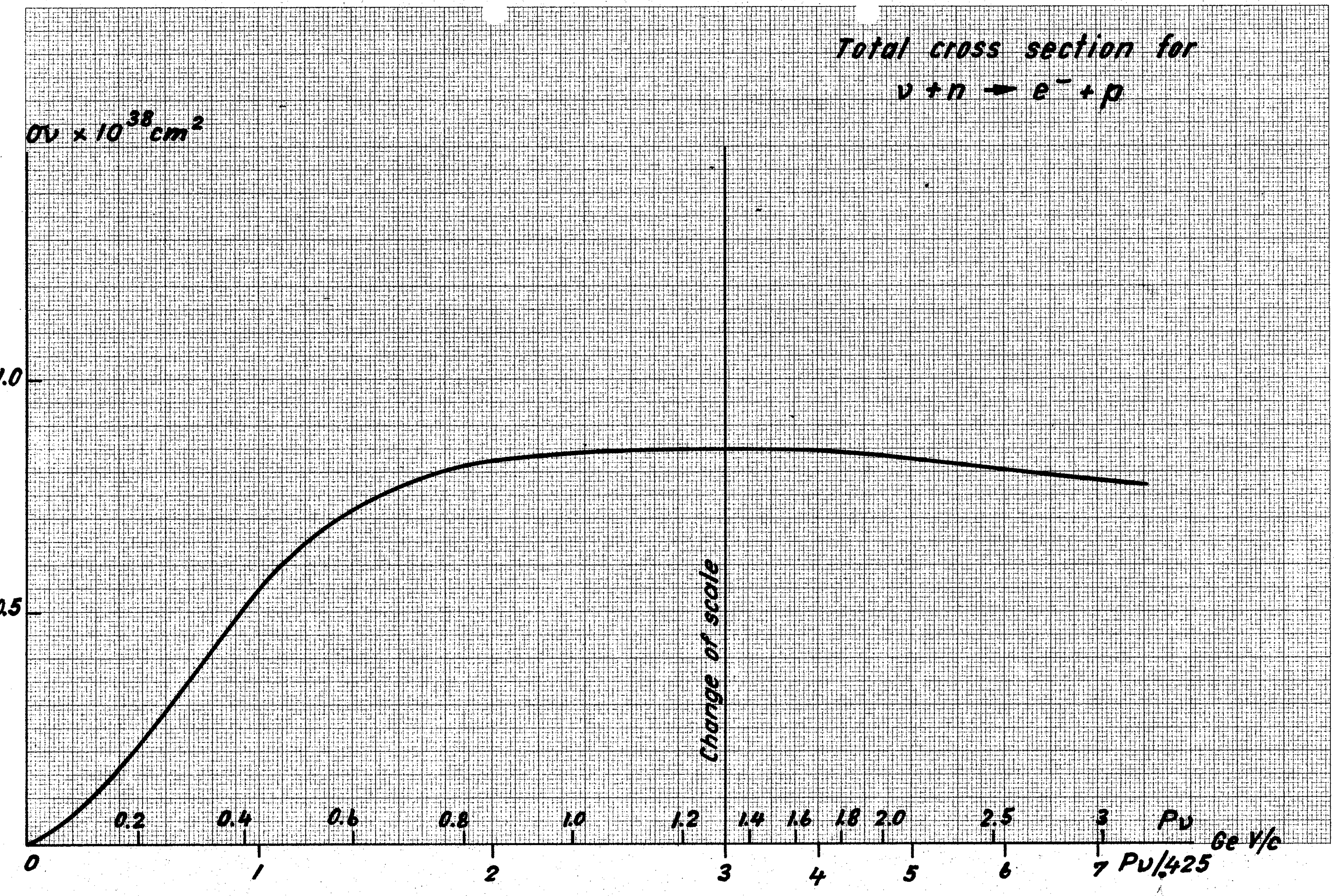

Total cross section for
ν + n → e⁻ + p
σν × 10³⁸ cm²
1.0
0.5
Change of scale
0.2
0.4
0.6
0.8
1.0
1.2
1.4
1.6
1.8
2.0
2.5
3
Pν
GeV/c
0
1
2
3
4
5
6
7
Pν/425

Fig. 2

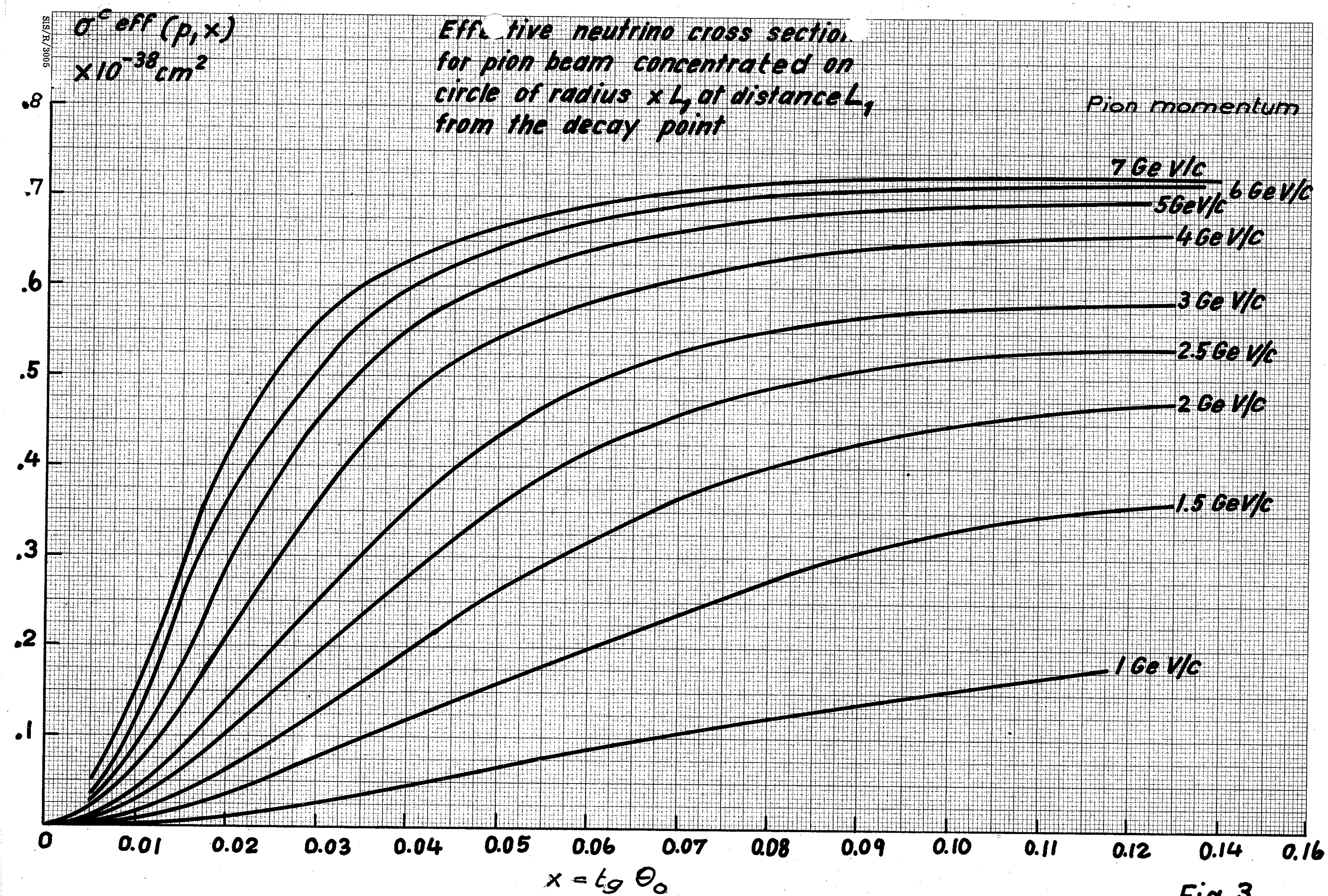

SIS/R/3005
σ^c eff (p, x)
×10^-38 cm^2
Eff tive neutrino cross sectio
for pion beam concentrated on
circle of radius x L1 at distance L1
from the decay point
Pion momentum
7 GeV/c
6 GeV/c
5GeV/c
4 GeV/c
3 GeV/c
2.5 GeV/c
2 GeV/c
1.5 GeV/c
1 GeV/c
.8
.7
.6
.5
.4
.3
.2
.1
0
0.01
0.02
0.03
0.04
0.05
0.06
0.07
0.08
0.09
0.10
0.11
0.12
0.14
0.16
x = tg Θo

Fig. 3

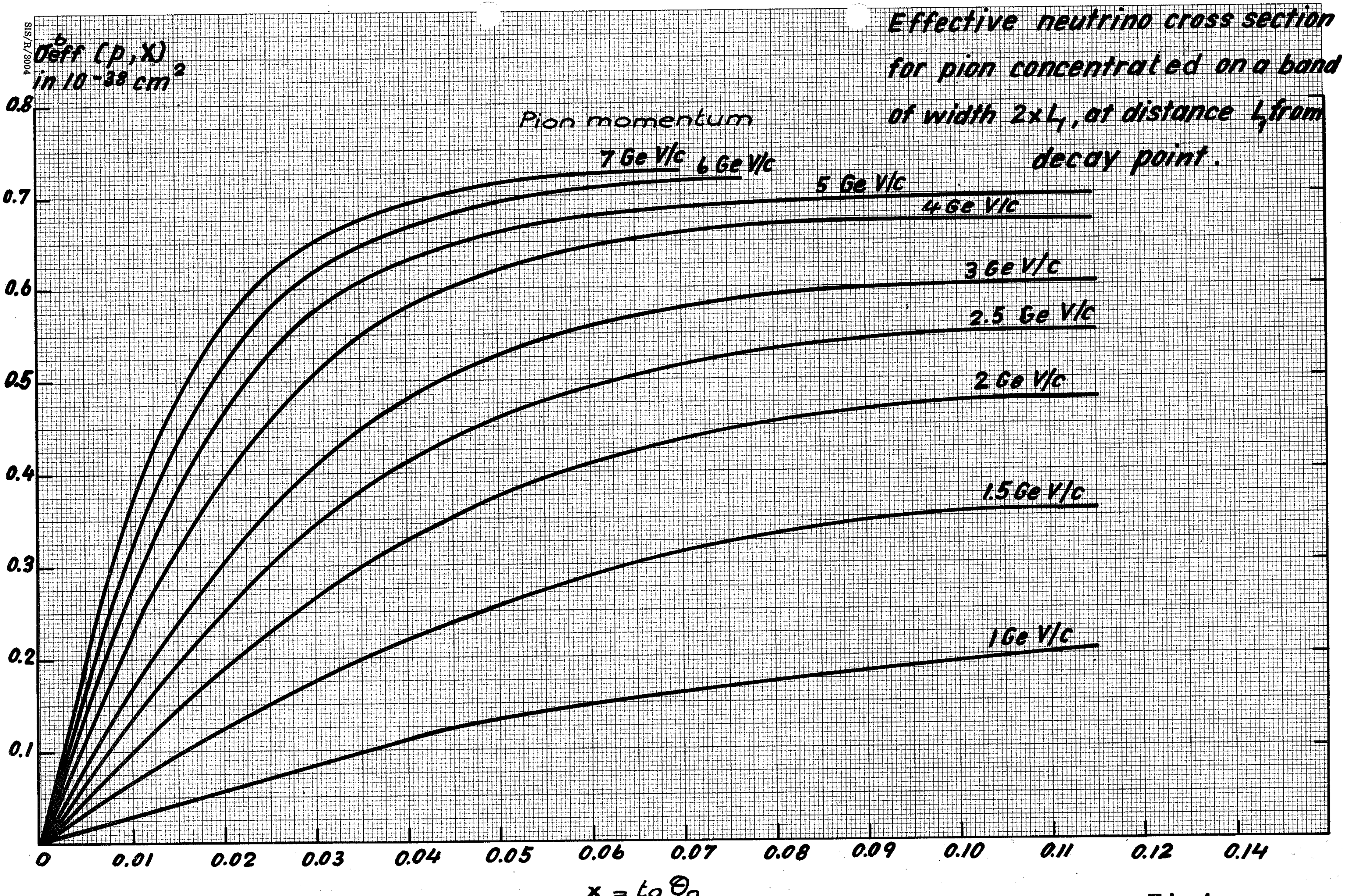

Effective neutrino cross section for pion concentrated on a band of width $2 x L_1$, at distance L_1 from decay point.
$\sigma^b_{eff}(p, X)$ in 10^{-38} cm^2
Pion momentum
7 GeV/c
6 GeV/c
5 GeV/c
4 GeV/c
3 GeV/c
2.5 GeV/c
2 GeV/c
1.5 GeV/c
1 GeV/c
0.8
0.7
0.6
0.5
0.4
0.3
0.2
0.1
0
0.01
0.02
0.03
0.04
0.05
0.06
0.07
0.08
0.09
0.10
0.11
0.12
0.14
$x = tg\,\theta_0$
SIS/R/3004

Fig. 4

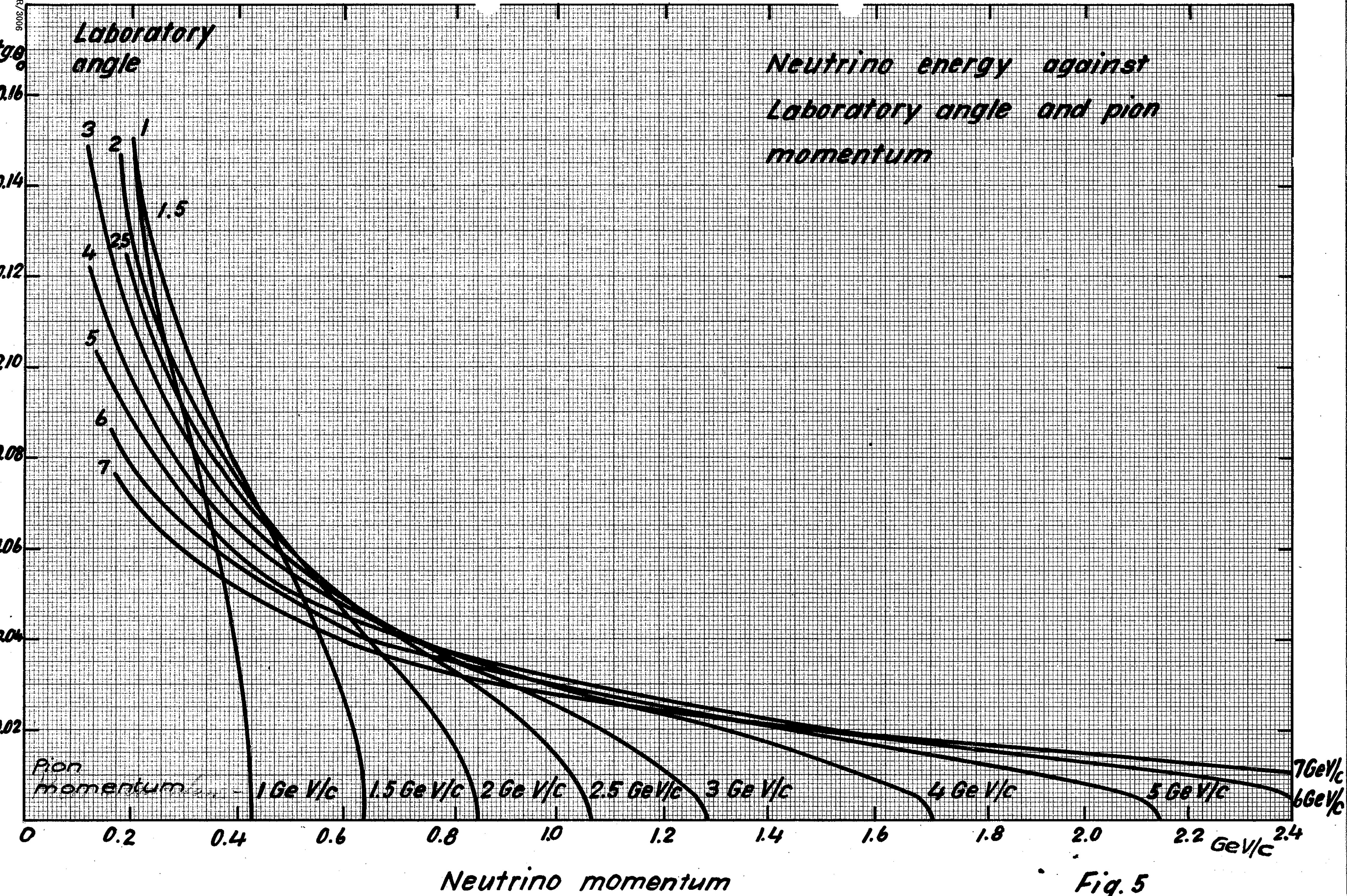
Laboratory angle
$tg\theta_0$
0.16
0.14
0.12
0.10
0.08
0.06
0.04
0.02
Neutrino energy against Laboratory angle and pion momentum
1
1.5
2
2.5
3
4
5
6
7
Pion momentum
1 Ge V/c
1.5 Ge V/c
2 Ge V/c
2.5 GeV/c
3 Ge V/c
4 Ge V/c
5 GeV/c
6GeV/c
7GeV/c
0
0.2
0.4
0.6
0.8
1.0
1.2
1.4
1.6
1.8
2.0
2.2
2.4
GeV/c
Neutrino momentum

Fig. 5

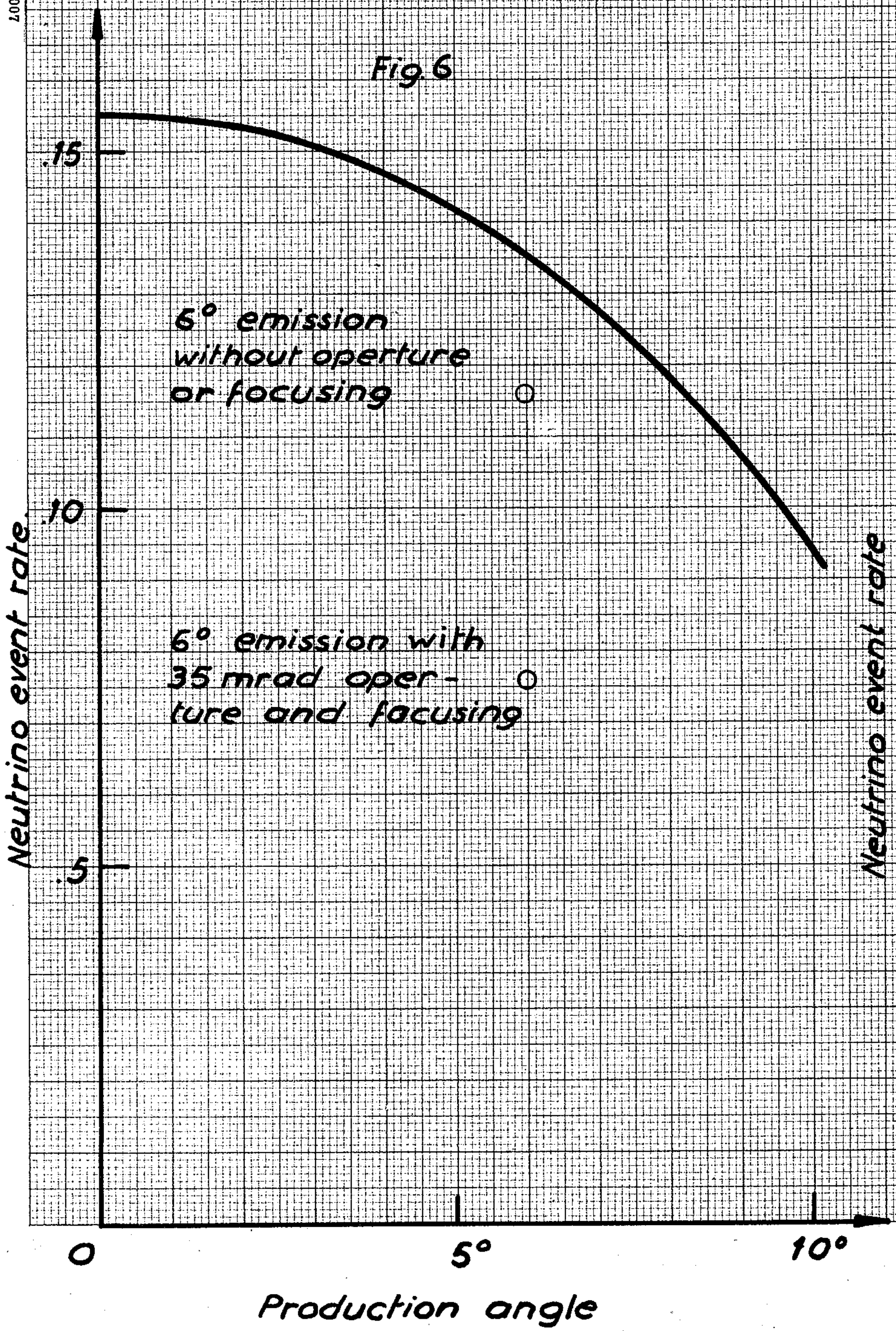
Fig.6
6° emission
without aperture
or focusing
6° emission with
35 mrad aper-
ture and focusing
.15
.10
.5
Neutrino event rate.
0
5°
10°
Production angle

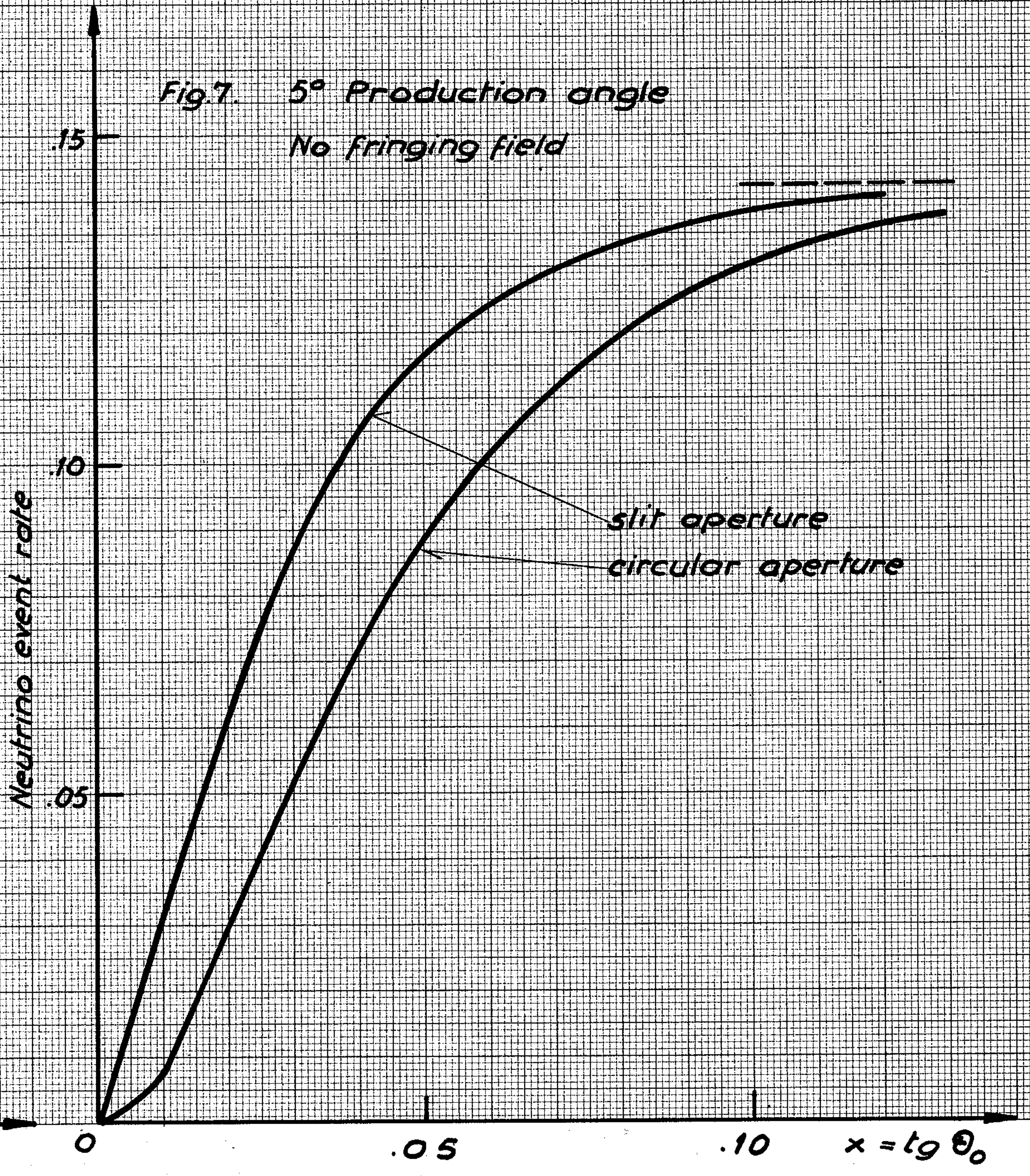
Fig.7. 5° Production angle
No fringing field
slit aperture
circular aperture
.15
.10
.05
Neutrino event rate
0
.05
.10
x = tg θ₀

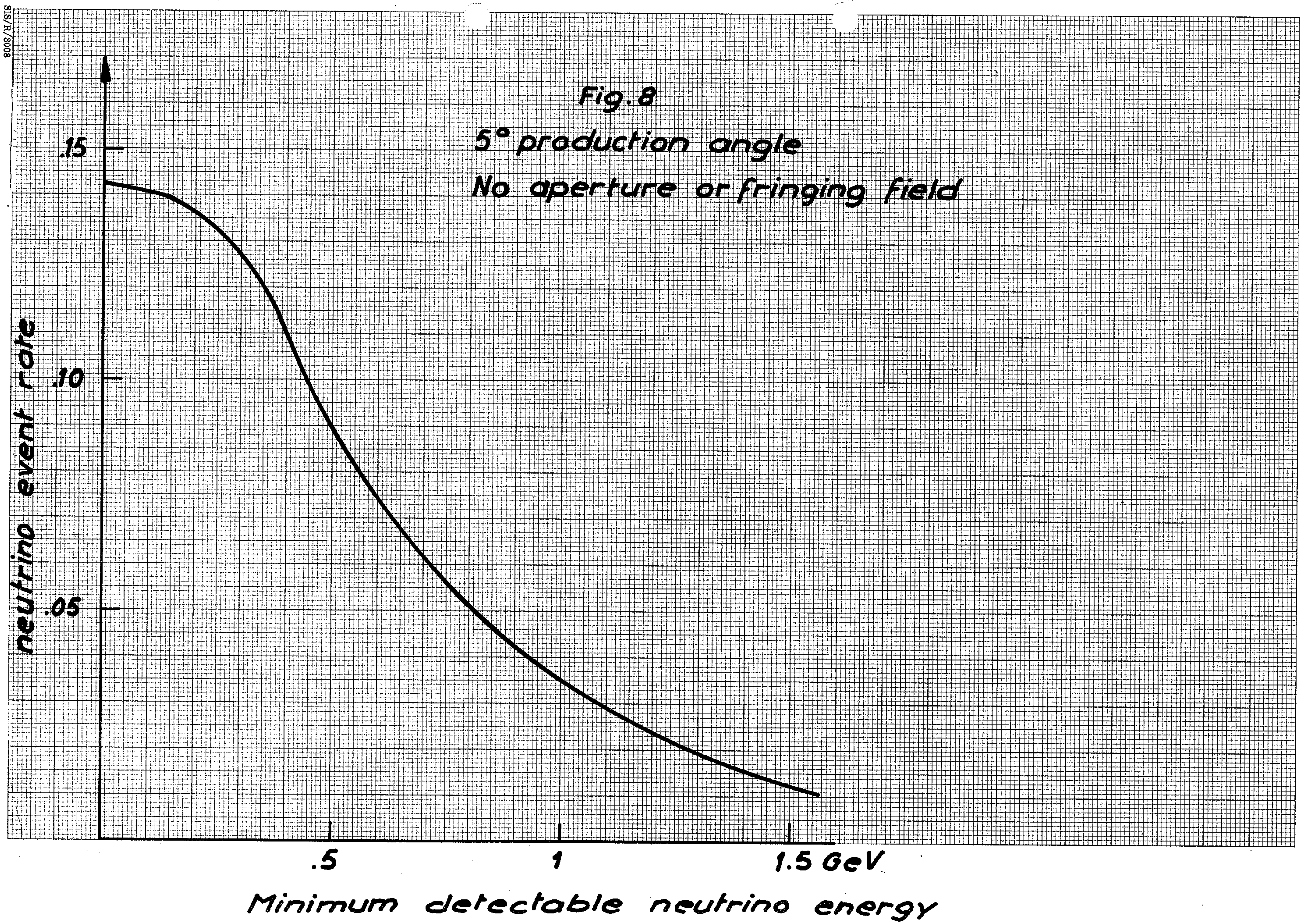
Fig. 8
5° production angle
No aperture or fringing field
.15
.10
.05
neutrino event rate
.5
1
1.5 GeV
Minimum detectable neutrino energy

SIS/R/3008